

# INFLUENCE OF CRACK OFFSET AND CRACK TIP DISTANCES ON THE INTERACTION OF MULTIPLE CENTRAL PARALLEL CRACKS IN A RECTANGULAR PLATE

Neeraj Bisht<sup>1</sup>, P C Gope<sup>2</sup>

<sup>1,2</sup> *Department of Mechanical Engineering, GB Pant University of Agriculture & Technology, (India)*

## ABSTRACT

*In the present work the finite element method has been employed to study the interaction of multiple cracks and the influence of the crack offset distance  $H$  and crack tip distance  $S$  on the interaction. The geometry chosen is a rectangular plate with central parallel cracks. The variations of stress intensity factors along with the stress distribution around the crack tips were studied with  $H$  &  $S$ . Due to the presence of a neighbouring crack, the intensification effect was observed. It was seen that the amount of interaction between the cracks depends to a great extent upon the parameter  $H$  &  $S$ . As the crack offset distance increases the interaction diminishes. An analysis of state of stress at the crack tip has also been done.*

**Keywords:** *Crack Interaction, Intensification, Finite Element Method, Stress Intensity Factor.*

## I. INTRODUCTION

The fracture mechanics theory can be used to analyze structures and machine components with cracks and to obtain an efficient design. The basic principles of fracture mechanics developed from studies of [1-3] are based on the concepts of linear elasticity.

The interaction between multiple cracks has a major influence on crack growth behaviours. This influence is particularly significant in stress corrosion cracking (SCC) because of the relatively large number of cracks initiated due to environmental effects. Wen Ye Tian and U Gabbert [4] have proposed pseudo – traction – electric – displacement –magnetic –induction method to solve the multiple crack interaction problems in magneto elastic material. Most of the real life situations have the problem of multiple cracks and so it becomes important to study this interaction for an array of cracks keeping this in mind interaction between two parallel cracks has been studied and a detailed analysis has been made into this aspect.

Since today, there have been over 20 approaches to calculate stress intensity factors. Some of these are the integral transform method [5], the Westergaard method [6], the complex variable function method [7], the singular equation integral method [8], conformal mapping [9], the Laurent series expansion [10], boundary collocation method [11], Green's function method [12], the continuous distribution dislocation method [13], the finite element method [14], the boundary element method [15], the body force method [16] and the displacement discontinuity method [17]. The solutions of many of the fracture mechanics problems have been compiled in data hand books for stress intensity factors [18] and [19].

The configuration of multiple cracks is so complicated that a solution may not be available from the handbooks and literatures. The above mentioned methods with analytical features, which are usually suitable for special cases or very simple crack configurations, are not sufficient to obtain reasonable results for general orientations due to many restrictions. In these cases numerical approaches are usually employed.

In the numerical approaches proposed so far FEM provides a very simple, effective and accurate technique for evaluation of fracture parameters.

The historical development of computational fracture mechanics is found in the works of Ingraffea and Wawrzynek [20] and Sinclair [21]. Sinclair [21] has presented an extensive review of stress intensity factor numerical prediction models. The advantages and disadvantages of using finite element in computational fracture mechanics have been well addressed by Ingraffea [22]. Miranda et al. [23] have discussed on the aspect of mesh refinement and associated error in computing stress intensity factors using finite element method. It has been reported that excessive mesh refinement may significantly degrade the calculation accuracy in crack problems. It was pointed out by Miranda et al. [23] that the ratio between the longest and shortest element edge lengths should be kept below 1600 to avoid calculation errors in SIF calculations. For meshes with length ratios higher than 1600, improved numerical methods to deal with ill conditioned matrices would be necessary to not compromise the calculation accuracy of the calculated SIF. Many works on mesh generation algorithms and new methods to improve the numerical computation of SIF values have been found in the works of Miranda et al. [24,25]. Recent studies show that the coefficients of higher order terms can also play an important role in the fracture process in notched or cracked structures. The recent studies show that in addition to the singular term, the higher order terms, in particular, the first non-singular stress term ( known as the T stress) may also have significant effects on the near notch tip stress field. The T-stress is considered in some studies as an auxiliary parameter for increasing the accuracy of the results for KI. Kim and Cho [26] for instance, showed that this non-singular term has noticeable effects on the size and shape of plastic zone near the notch tip. Ayatollahi and colleagues demonstrated that the first non-singular term may have considerable contributions to the stress components around the notch tip and also on the fracture resistance of notched components under mode I loading [27, 28 and 29].

## II. FINITE ELEMENT MODELLING

The numerical simulations run by means of the FE software ANSYS are conducted to determine the stress intensity factors of two central parallel cracks. The specimen in fig.1 is schematized by a 2D model. The specimen thickness in FE analysis was kept 1.0 mm, and the model was studied in plane strain condition. Isoperimetric quadrilateral elements (PLANE 82) with singularity elements at and around the crack tip having 8 nodes are used throughout the analysis shown in Fig. 2. The radius of first row of elements is taken as  $a/8$ , where  $a$  is the half crack length and the radius ratio (second row/first row) is adjusted automatically. The number of elements around the circumference is taken as 32 for full crack model. The FE modelling parameters are selected on the basis of the error analysis presented in Fig. 3 for two edge cracks. This is studied by varying the radius of the first row of the crack tip element and number of elements in the first row. To analyze the SIF calculation, the density of the FE mesh is modified by varying the number of the elements of the first row as 16, 20, 24, 32 and 40 keeping the radius of the first row as  $a/8$ ,  $a$  is the crack length and taken as 10 mm. Also, the radius of the first row ( $a/n$ ) around the crack tip is varied, taking  $n$  8, 10, 12, 16

and 20 with 32 number of elements. FE analyses are performed for each of the ten meshing strategies, and K values are computed. Theoretically KI is computed from the relation given for two collinear edge cracks [30]. It is found that the KI calculation errors stay below 0.8% for all meshing strategies. Figs. 3(a-b) show variation of the normalized KI (FE based computation to the actual (theoretical) Mode I SIF) for different mesh configuration, as a function of the number of crack face elements and normalized first crack tip radius. It is clearly seen from Fig. 3 that, on average, the calculation with the radius of first element as 1.25 mm (i.e.  $8/a=1.25$ ) and number of elements around the crack tip as 16 yields least error i.e. closest to unity amongst the other mesh configurations. For the numerical simulation, a uniform pressure intensity of 1.0 MPa is applied to the upper and lower edges in the vertical direction (y axis). The displacements in the horizontal direction (x axis) and rotations are prevented. The mechanical properties used for FE analysis are  $E=70$  GPa and Poisson's ratio 0.33. The mode I and mode II stress intensity factors are computed from the following relations:

$$K_I = \sqrt{2\pi} \frac{G}{k} \frac{|\Delta v|}{\sqrt{r}} \quad (1)$$

$$K_{II} = \sqrt{2\pi} \frac{G}{1+k} \frac{|\Delta u|}{\sqrt{r}} \quad (2)$$

Where  $\Delta v$ ,  $\Delta u$  and  $\Delta w$  are the motions of one crack face with respect to the other.

$k= 3-4\nu$  if plane strain or axisymmetric;  $(3-\nu) (1+\nu)$  if plane stress; where  $\nu$  is Poisson's ratio.

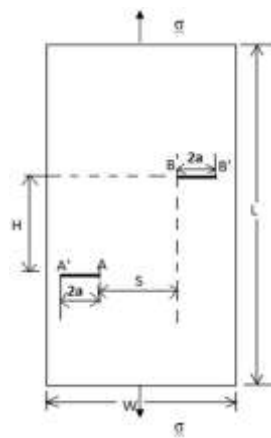


Fig. 1 Specimen Geometry

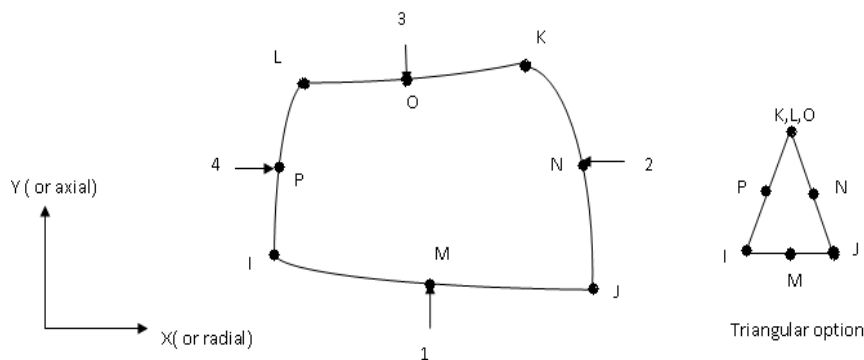
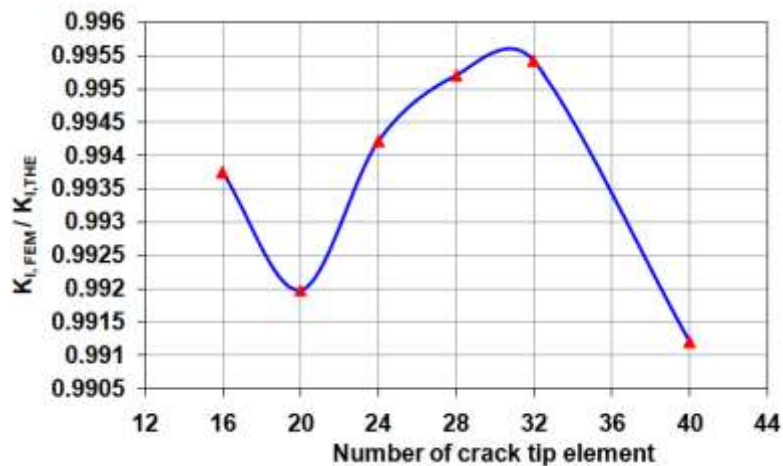
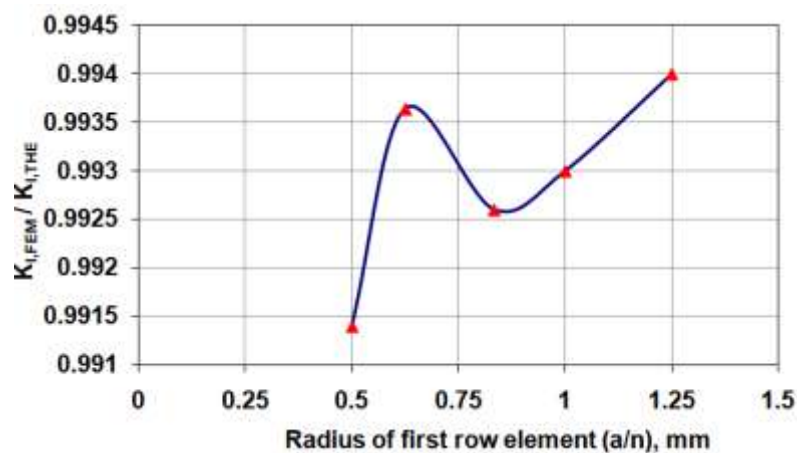


Fig.2 Plane 82 Element with 8-Nodes



**Fig. 3(A) Variation of Stress Intensity Factor With Number of Crack Tip Elements**



**Fig. 3(B) Variation of Stress Intensity Factor With Radius of First Row of Elements,  $K_{I,FEM}$  And  $K_{I,THE}$  are Finite Element and Theoretical Based Computations of Mode I Stress Intensity Factor**

Mode III stress intensity factor in the present investigation is not considered because the thickness of the plate in FE analysis is taken as unity. However, the three dimensional effect or plate thickness effect on the stress intensities can be seen in the works of Kotousov et al. [31,32].

In the present FE computation, out of balance convergence and degree of freedom increment convergence criteria are adopted. The tolerance level kept is 0.001. These criteria are well documented in the ANSYS manual [33].

### III. RESULTS & DISCUSSIONS

The effect of crack tip and crack offset distance of two central parallel cracks are discussed in this section.

#### 3.1 Stress Intensity Factor

Figs. 4 to 12 show the relationship between normalised stress intensity factors and relative positions of two central parallel cracks. Mode I and mode II SIF's are normalised with  $K_0$  for single central cracked geometry given by [Kumar [2009]]:

$$K_0 = \sigma \sqrt{\pi a} f(a/w) \quad (1)$$

where

$$f(a/w)=1 + 0.128(a/w) - 0.288(a/w)^2 + 1.523(a/w)^3 \quad (2)$$

Here  $a = 4$  mm,  $w = W/2 = 40$  mm

$$f(a/w) = 1.01007 \quad (3)$$

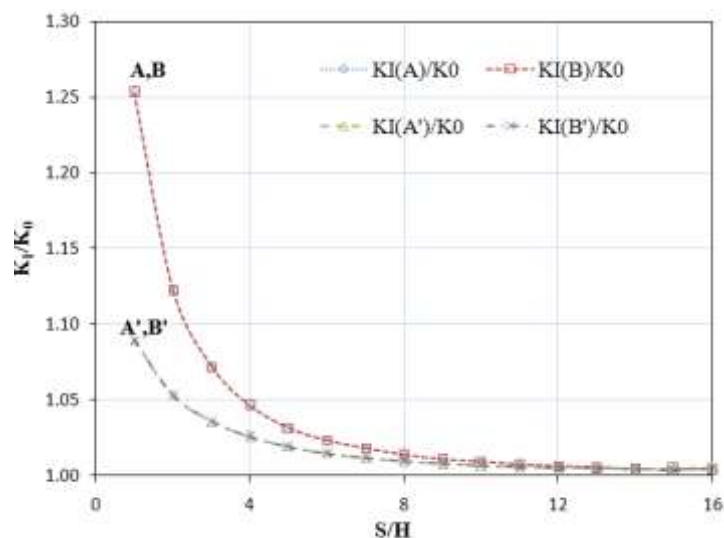
hence,  $K_0 = 358.06 \text{ MPa}\sqrt{\text{mm}}$

$K_0$  is the stress intensity factor for single central crack of size  $2a$  in a finite width plate. Therefore unity in the normalised stress intensity factor corresponds to the condition of zero interaction. As seen in fig. 4 and 7, strong interaction appears at the inner crack tip, when the cracks are in the range  $S/H \leq 8$  mm position for  $H = 2$  mm and  $S/H \leq 6$  mm for  $H = 4$  mm. The difference between SIF's at inner and outer crack tip becomes almost insignificant beyond  $S/H = 12$  mm.

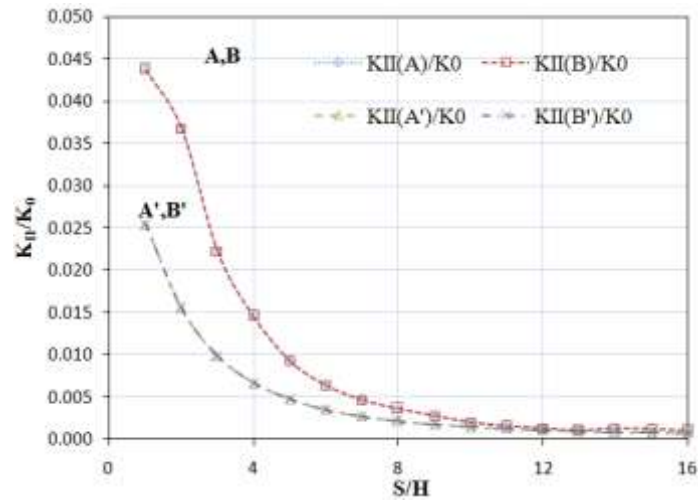
At the outer crack tip as shown in fig 4 and 7, little interaction effect appears when the cracks are very close to each other. It is observed that for  $H \leq 4$  mm, maximum of 10% increase in mode I SIF is seen as compared to single central crack.

Fig. 5 and 8 shows the variation of mode II SIF's for both inner and outer crack tips for  $H=2$  mm and 4 mm respectively and it can be seen that there is an interaction on mode II SIF and its value is about 4.5% of mode I SIF at outer crack tip for  $H = 2$  mm and  $H = 4$  mm and thereafter it reduces to negligible interaction. It is seen that the interaction is higher for inner crack tip than the outer one.

Figs. 10 and 11 shows that two type of interactions occur. When  $H \geq 25$  mm, a relaxation (less than unity in normalised SIF) and for  $H < 25$  mm intensification (higher than unity) exists. Fig.11 also reveals that the difference of SIF's for inner and outer crack tip is very small when  $H \geq 25$  mm, but the difference increases to about 10% beyond  $H=5$  mm. Thereafter the difference between SIF at inner and outer crack tip remains constant. Similar trends are seen for both  $K_I$  and  $K_{II}$ .



**Fig. 4 Variation of Normalized S.I.F.'s For Central Parallel Crack Specimen C1 (H=2 Mm) With S/H**



**Fig.5** Variation of Normalised SIF's for Central Parallel Crack Specimen C1 (H=2 Mm) With S/H

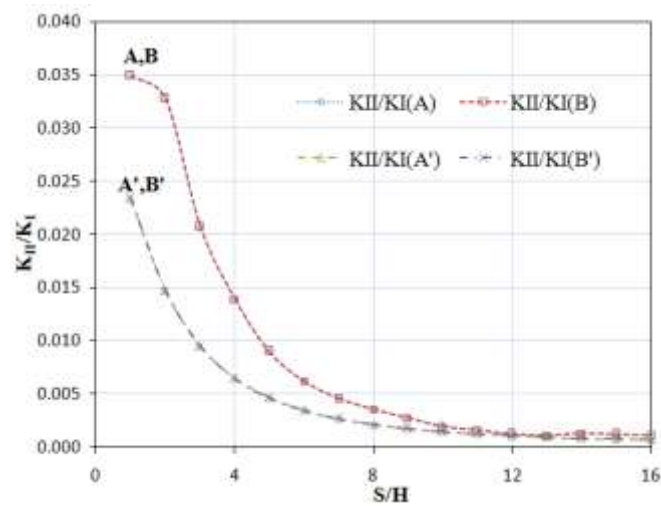


**Fig. 6** Variation of Normalized S.I.F's for Central Parallel Crack Specimen C1 (H=2 Mm) With S/H

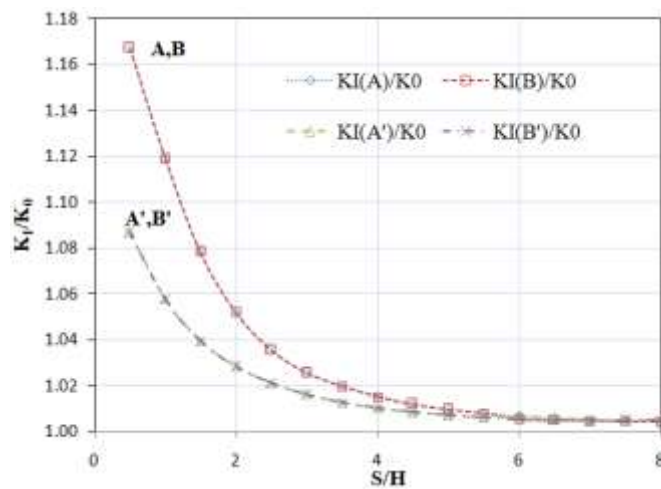


**Fig. 7** Variation of Normalized S.I.F's for Central Parallel Crack Specimen C1 (H=4 Mm) With S/H

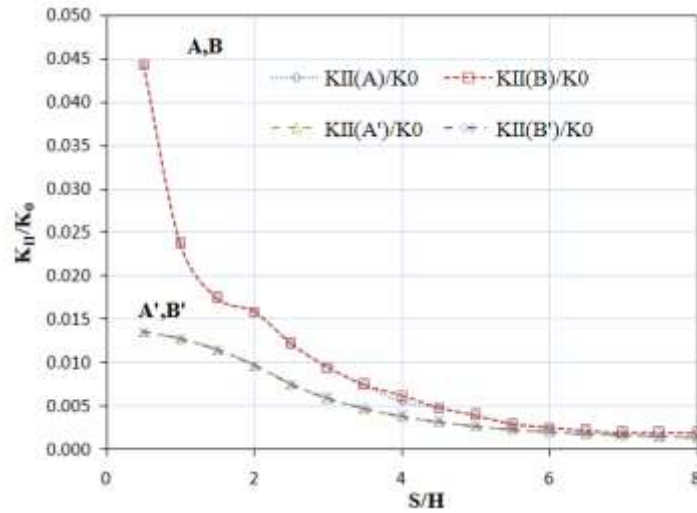


**Fig. 8** Variation of Normalized S.I.F's for Central Parallel Crack Specimen C1 (H=4 Mm) With S/H

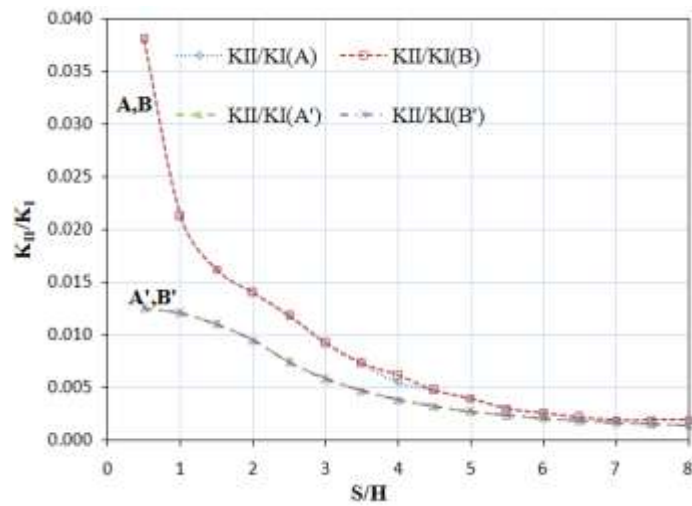


**Fig. 9** Variation of Normalized S.I.F's for Central Parallel Crack Specimen C1 (H=4 Mm) With S/H

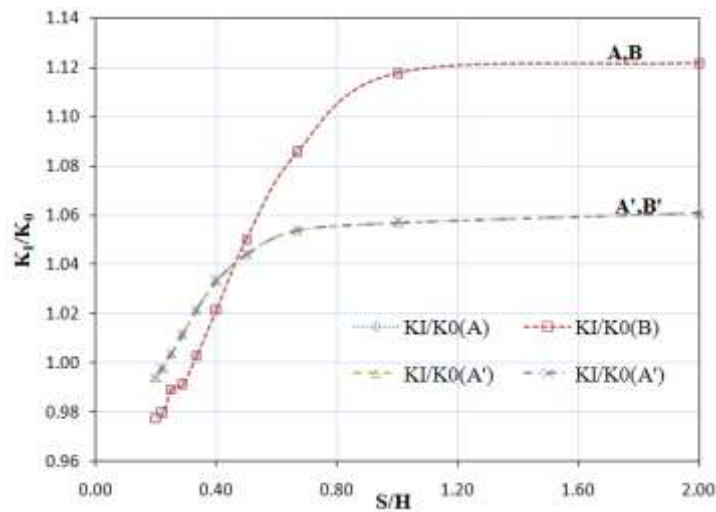


**Fig. 10** Variation of Normalized S.I.F's for Central Parallel Crack Specimen C1 (S=4 Mm) With S/H

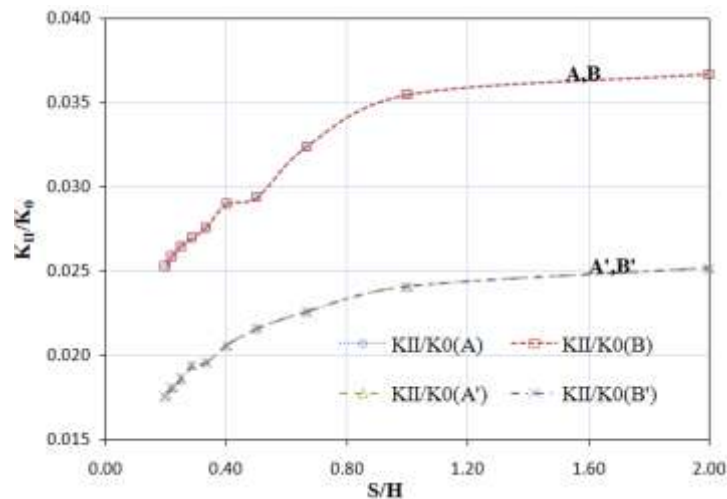


**Fig. 11 Variation of Normalized S.I.F's for Central Parallel Crack Specimen C1 (S=4 Mm) With S/H**

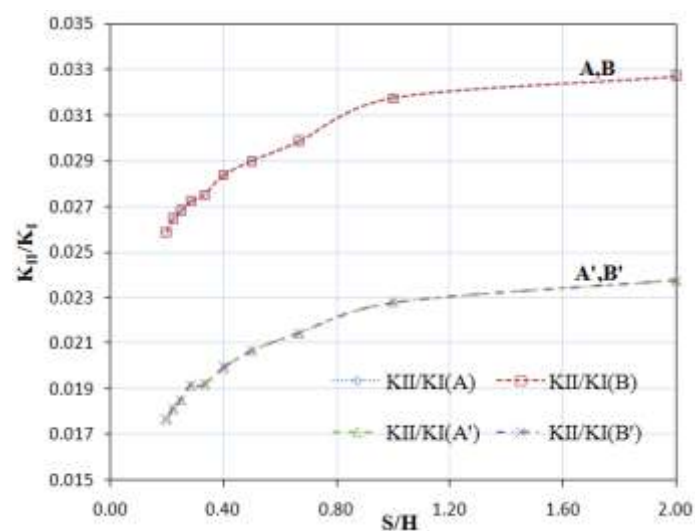


**Fig. 12 Variation of Normalized S.I.F's for Central Parallel Crack Specimen C1 (S=4 Mm) With S/H**

## 2.2 Analysis of state of Stress

The two dimensional finite element model presented in this work has been used to investigate the state of stress around the crack tip in plane strain condition. The state of stress at a radial distance  $r$  from the crack tip is schematically shown in Fig. 13. The results obtained for different crack configurations are presented in Figs.12 to 19. The stresses computed for double edge cracks are normalized with  $\sigma_y$  which is the yield strength of the material.

Fig. 14-16 shows the variation of  $\sigma_{xx}$ ,  $\sigma_{yy}$  and  $\tau_{xy}$  around the crack tip element at a radial distance of 0.5 mm for crack specimen for different crack tip distance  $S = 2$  mm, 6 mm and 12 mm. Fig. shows that significant variation in  $\sigma_{yy}$  is observed between  $S = 2$  mm and 6 mm or 12 mm. For  $S = 2$  mm,  $\sigma_{yy}$  at the crack tip is almost 2.5 times the yield strength of the material whereas for  $S = 6$  mm or 12 mm, the value of  $\sigma_{yy}$  remains less than two times of the yield strength of the material.  $\sigma_{xx}$  remains less than yield strength of the material for all  $S$  values. The shearing stress  $\tau_{xy}$  are greater than zero and are 49.101 MPa, 9.1250 MPa and 13.42 MPa for  $S = 2$  mm, 6 mm and 12 mm respectively. From the distribution of stresses, it can be inferred that crack tip distance

for specimen geometry has inverse effect i.e. for smaller values of S, the mode I and mode II SIF should be more as compared to higher values of S.

The effect of H on stress distribution around the crack tip elements of specimen configuration are shown in Fig. 17-19 for S = 4 mm. Similar trend as seen for different S values are observed for crack offset distance H also. The stresses are higher for smaller values of H as compared to higher values of H. It means that when cracks are close to each other the higher state of stress is yielded at the crack tip and as S or H increases stress reduces. This indicates that both S and H have significant effect on the state of stress at the crack tip and hence on the stress intensity factors.

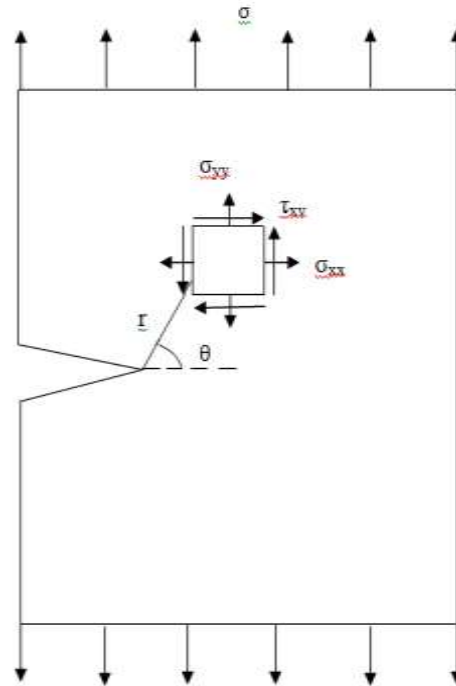


**Fig. 13 Schematic Representation of State of Stress of a Cracked Body**

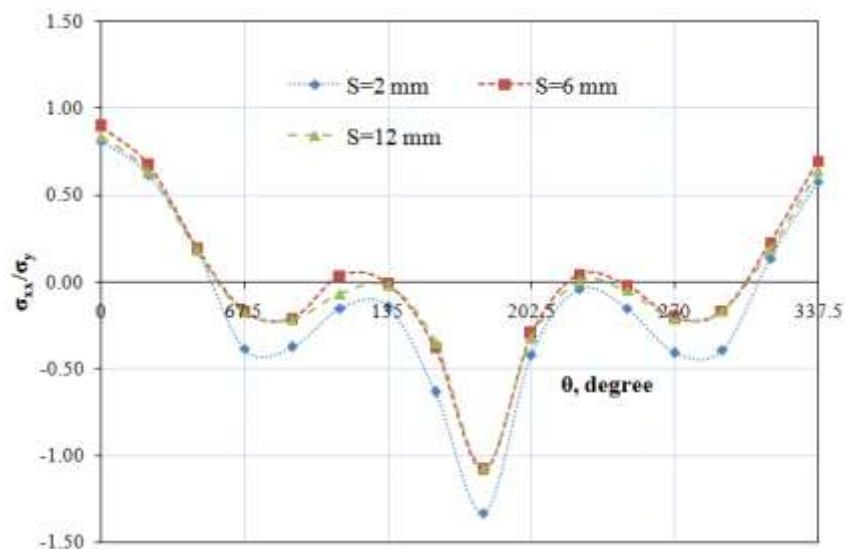


**Fig. 14 Variation of  $\Sigma_{xx}/\Sigma_y$  with S for Specimen Geometry C1 (H=2 Mm)**

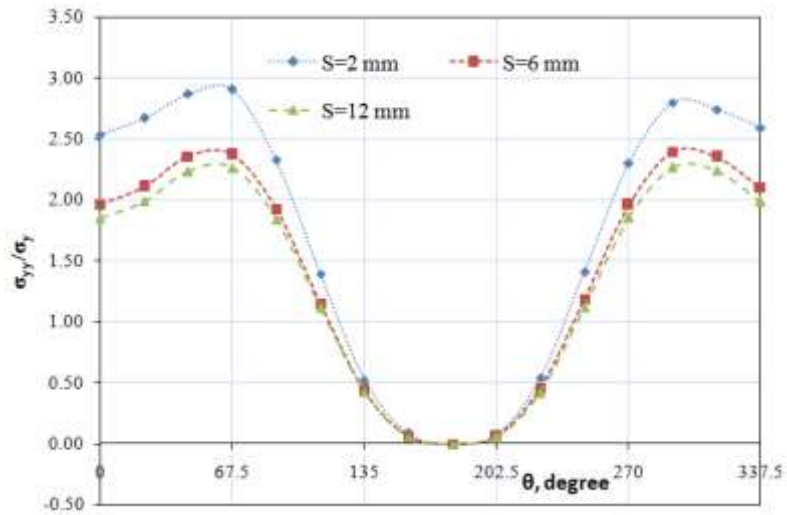


Fig.15 Variation of  $\Sigma_{yy}/\Sigma_y$  with S for Specimen Geometry C1 (H=2 Mm)

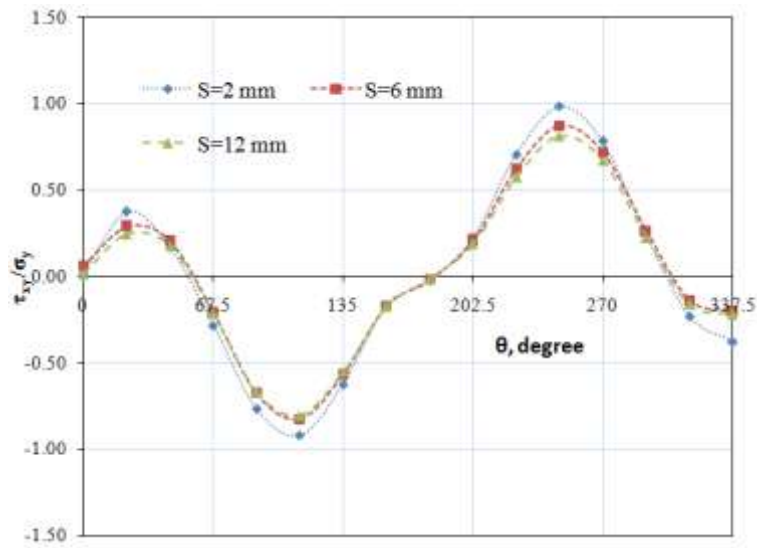


Fig.16 Variation of  $T_{xy}/\Sigma_y$  with S for Specimen Geometry C1 (H=2 Mm)

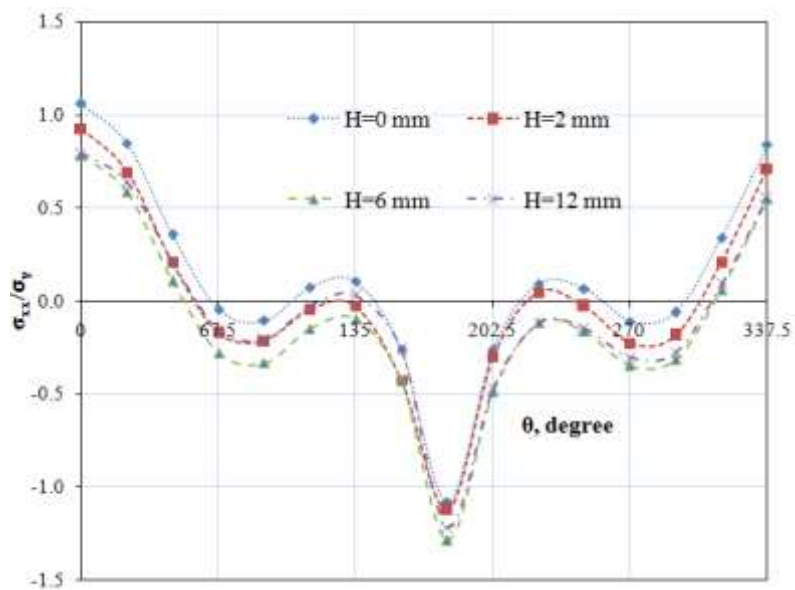
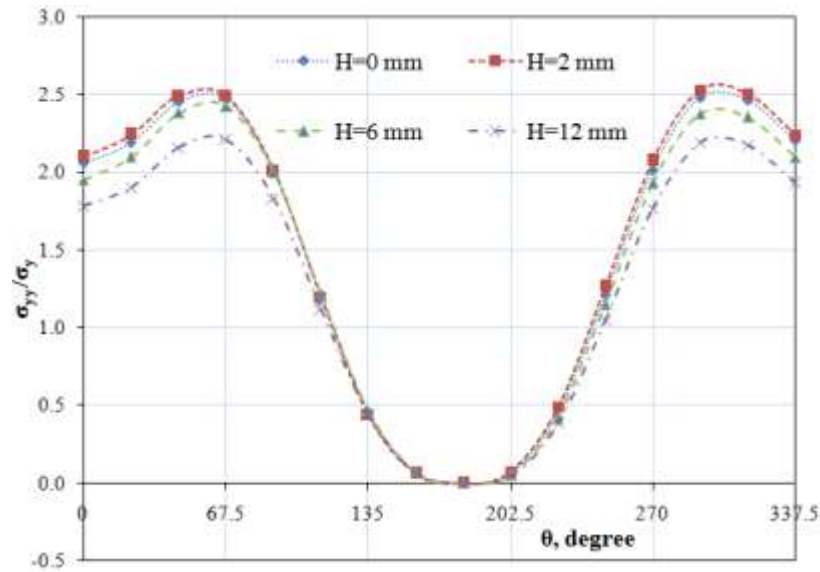
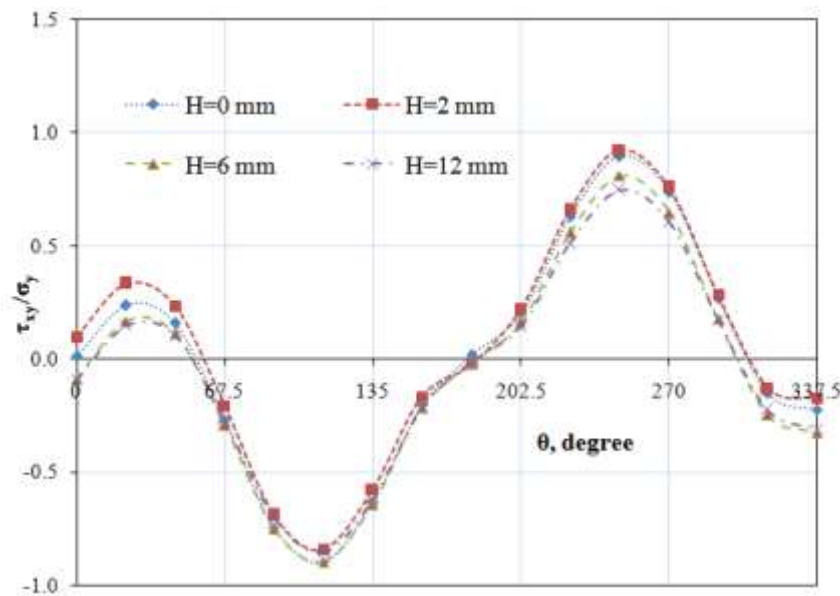


Fig. 17 Variation of  $\Sigma_{xx}/\Sigma_y$  with H for Specimen Geometry C1(S=4 Mm)



**Fig. 18 Variation of  $\Sigma_{yy}/\Sigma_y$  with H for Specimen Geometry C1(S=4 Mm)**



**Fig. 19 Variation of  $T_{xy}/\Sigma_y$  with H for Specimen Geometry C1(S=4 Mm)**

### III. CONCLUSIONS

1. There is a profound effect of presence of a neighbouring crack on the fracture parameters.
2. Intensification effect is observed for mode I stress intensity factor.
3. Mode II stress intensity factor which was otherwise absent for a single crack comes into existence due to the interaction.
4. The stress intensity factors were greater for the neighbouring crack tips.
5. The interaction ceases to exist as cracks move farther away from each other.
6. Mode I stress intensity factor is predominant for all crack orientations.
7. The vulnerability of a structure increases due to the presence of multiple neighbouring cracks.

## REFERENCES

- [1] C.E. Inglis, Stresses in a plate due to the presence of cracks and sharp corners, Transactions-Institute of Naval Architect, 55, 1913, 219-230.
- [2] A.A. Griffith, The phenomenon of rupture and flow in solids, Trans. Royal Soci. London, 221, 1920, 163-198.
- [3] H. M. Westgaard, Bearing pressure and cracks, Journal of Applied Mathematics and Mechanics, 6, 1939, 49-53.
- [4] T. Wen-Ye, U. Gabbert, Multiple crack interaction problems in magneto-electrostatic solids, European Journal of Mechanics and Solids, 23, 2004, 599.
- [5] I. N. Sneddon, M., Lowengrub, Crack Problems in Classical Theory of Elasticity (Wiley, New York, 1969).
- [6] H. M. Westergaard, Bearing pressure and cracks, ASME Journal of Applied Mechanics, 6, 1939, 49-53.
- [7] N. I. Muskhelishvili, Some Basic Problems of Mathematical Theory of Elasticity (Holland, Noordhoff: 1977).
- [8] F. Erdogan, Stress Intensity Factors, ASME Journal of Applied Mechanics, 50, 1983, 992-1002.
- [9] O. L. Bowie, Analysis of an infinite plate containing radial cracks originating at the boundary of an internal circular hole, Journal of Mathematical Physics, 25, 1956, 60-71.
- [10] M. Isida, Stress intensity factors for the tension of an eccentrically cracked strip, ASME Journal of Applied Mechanics, 33, 1966, 674-675.
- [11] M. L. Williams, On the stress distribution at the base of a stationary crack, ASME Journal of Applied Mechanics, 24, 1957, 104-114.
- [12] G. C. Sih, P. C. Paris, F. Erdogan, Crack tip stress intensity factors for plane extension and plate bending problems, ASME Journal of Applied Mechanics, 29, 1962, 306-314.
- [13] J. D. Eshelby, F. C. Franck, F. R. N. Nabarro, The Equilibrium of Linear Arrays of Dislocations, Philosophical Magazine, 42, 1951, 351-364.
- [14] V. B. Watwood, The Finite Element Method for Prediction of Crack Behaviour, Nuclear Engineering Design, 11, 1969, 323-332.
- [15] T. A. Cruse, Numerical Solutions in Three Dimensional Elastostatics, International Journal of Solids and Structures, 5, 1969, 1259-1274.
- [16] H. Nisitani, Solutions of Notch Problems by the Body Force Method in Fracture Mechanics (Holland, Noordhoff International: 1978).
- [17] S. L. Crouch, A. M. Starfield, Boundary Element Method in Solid Mechanics, with Application in Rock Mechanics and Geological Mechanics (London, George Allen & Unwin: 1983).
- [18] L. P. Pook, Stress intensity factor expressions for regular crack arrays in pressurised cylinders, Fatigue and Fracture of Engineering Materials and Structures, 13, 1990, 135-143.
- [19] David Percy Rooke, David John Cartwright, Compendium of stress intensity factors Great Britain, (Ministry of Defence, Procurement Executive, 1976).
- [20] A.R. Ingraffea, P.A. Wawrzynek, in: R.d.B.a.H. Mang (Ed.), Comprehensive Structural Integrity (Oxford, Elsevier Science Ltd.: 2003).

- [21] G. Sinclair, Stress singularities in classical elasticity—II: Asymptotic identification, *Applied Mechanics Reviews*, 57, 2004, 251–298.
- [22] A.R. Ingraffea, *Encyclopedia of Computational Mechanics* (NJ, John Wiley and Sons: 2004).
- [23] Antonio Carlos de Oliveira Miranda, Marco Antonio Meggiolaro, Luiz Fernando Martha, Jaime Tupiassú Pinho de Castro, Stress intensity factor predictions: Comparison and roundoff error, *Computational Materials Science*, 53, 2012, 354–358.
- [24] A.C.O. Miranda, M.A. Meggiolaro, J.T.P. Castro, L.F. Martha, T.N. Bittencourt, Fatigue life and crack path predictions in generic 2D structural components, *Engineering Fracture Mechanics*, 70, 2003, 1259–1279.
- [25] Antonio Carlos de Oliveira Miranda, Marco Antonio Meggiolaro, Jaime Tupiassú Pinho de Castro, Luiz Fernando Martha, Fatigue life prediction of complex 2D components under mixed-mode variable amplitude loading, *International Journal of Fatigue*, 25, 2003, 1157–1167.
- [26] J. K. Kim, S. B. Cho, Effect of second non-singular term of mode I near the tip of a V notched crack, *Fatigue and Fracture of Engineering Materials and Structures*, 2, 2009, 346–356.
- [27] M. R. Ayatollahi, M. Nejati, Determination of NSIFs and coefficients of higher order terms for sharp notches using finite element method, *International Journal of Mechanical Sciences*, 53, 2011, 164-177.
- [28] M. R. Ayatollahi, M. Deghany, On T-stresses near V-notches, *International Journal of Fracture*, 165, 2010, 121-126.
- [29] M. R. Ayatollahi, M. Nejati, Experimental evaluation of stress field around the sharp notches using photoelasticity, *Materials and Design*, 32, 2011, 561-569.
- [30] Kumar Prashant, *Elements of Fracture Mechanics* (New Delhi, McGraw-Hill Book Company: 2009).
- [31] Andrei Kotousov, Filippo Berto, Paolo Lazzarin, Fabio Pegorin, Three dimensional finite element mixed fracture mode under anti-plane loading of a crack, *Theoretical and Applied Fracture Mechanics*, 62, 2012, 26–33.
- [32] Andrei Kotousov, Effect of plate thickness on stress state at sharp notches and the strength paradox of thick plates, *International Journal of Solids and Structures*, 47, 2010, 1916–1923.
- [33] ANSYS Manual Release 8.0